

Forced Convection Heat Transfer of Nanofluids in a Porous Channel

M. J. Maghrebi · M. Nazari · T. Armaghani

Received: 3 November 2011 / Accepted: 6 February 2012 / Published online: 22 February 2012
© Springer Science+Business Media B.V. 2012

Abstract This article is concerned with the effects of flow and migration of nanoparticles on heat transfer in a straight channel occupied with a porous medium. Investigation of force convective heat transfer of nanofluids in a porous channel has not been considered completely in the literature and this challenge is generally considered to be an open research topic that may require more study. The fully developed flow and steady Darcy–Brinkman–Forchheimer equation is employed in porous channel. The thermal equilibrium model is assumed between nanofluid and solid phases. It is assumed that the nanoparticles are distributed non-uniformly inside the channel. As a result the volume fraction distribution equation is also coupled with governing equations. The effects of parameters such as Lewis number, Schmidt number, Brownian diffusion, and thermophoresis on the heat transfer are completely studied. The results show that the local Nusselt number is decreased when the Lewis number is increased. It is observed that as the Schmidt number is increased, the wall temperature gradient is decreased and as a consequence the local Nusselt number is decreased. The effects of Lewis number, Schmidt number, and modified diffusivity ratio on the volume fraction distribution are also studied and discussed.

Keywords Nusselt number · Particle migration · Brownian motion · Thermophoresis

List of Symbols

x, y Cartesian coordinate (m)
 u Axial velocity (ms^{-1})
 K Permeability (m^2)
 Da Darcy number

M. J. Maghrebi
Department of Mechanical Engineering, Ferdowsi University of Mashhad, Mashhad, Iran

M. Nazari (✉) · T. Armaghani
Department of Mechanical Engineering, Shahrood University of Technology,
P.O. Box: 3619995161, Shahrood, Iran
e-mail: nazari_me@yahoo.com

P	Pressure (Nm^{-2})
T	Temperature (K)
D_T	Thermophoretic diffusion coefficient ($\text{m}^2 \text{s}^{-1}$)
D_B	Brownian diffusion coefficient ($\text{m}^2 \text{s}^{-1}$)
H	Half length of channel
t	Time (s)
Re	Reynolds number
Pr	Prandtl number
N_{BT}	Brownian motion parameter
k	Thermal conductivity ($\text{Wm}^{-1} \text{K}^{-1}$)
Le	Lewis number
Sc	Schmidt number

Greek Letters

μ	Viscosity ($\text{kg m}^{-1} \text{s}^{-1}$)
ε	Porosity
ρ	Density (kgm^{-3})
φ	Volume fraction
σ	Thermal capacity ratio
Δ	Inertia parameter
α	Effective thermal diffusivity ($\text{m}^2 \text{s}^{-1}$)
τ	Modified diffusivity ratio

Subscripts

f	Fluid
m	Porous media
p	Particle
c	Reference
*	Dimensionless variables

1 Introduction

Nanofluid, a name conceived by Choi (1995) in Argonne National laboratory, are fluids consisting of solid nanoparticles with size less than 100 nm suspended with solid volume fraction typically less than 4%. Nanofluid can enhance heat transfer performance compared to pure liquids. Nanofluids can be used to improve thermal management system in many engineering application such as transportation, micromechanics and instrument, HVAC system and cooling devices. Recently, many investigators studied nanofluid convective heat transfer in different geometry both numerically and experimentally (Maiga et al. 2004; Heris et al. 2006; Duangthongsuk and Wongwises 2009; Santra et al. 2009; Nguyen et al. 2009). For numerical simulation, two approaches have been adopted in the literature to investigate the heat transfer characteristics of nanofluids, single phase model and two phase model. Another approach is to adopt the Boltzmann theory (Wang and Mujumdar 2007). In single phase model, a uniform volume fraction distribution is assumed for nanofluids. In other words, the viscosity and thermal conductivity of nanofluids are formulated by volume fraction and nanoparticle size then continuity, momentum and energy equations are solved for nanofluids. In two phase model,

the volume fraction distribution equation is added to other conservation equations. Many investigators used single and two phase models for investigating the flow and heat transfer of nanofluids (Behzadmehr et al. 2007; Lee and Mudawar 2007; Mirmasoumi and Behzadmehr 2008).

Buongiorno (2006) introduced seven slip mechanisms between nanoparticles and the base fluid. He showed that the Brownian motion (movement of nanoparticles from high concentration site) and thermophoresis (movement of nanoparticles from the high temperature site to the low temperature site) have effected significantly in the laminar forced convection of nanofluids. Based on this finding, he developed non-homogeneous two-component equations in nanofluids. Heyhat and Kowsary (2010) used Buongiorno's equations for investigating the effect of particles migration on flow and convective heat transfer of nanofluids flowing through the circular pipe. Results show that the non-uniform distribution leads to a higher heat transfer coefficient while the wall shear stress is decreased. Therefore, the particle migration can play an important role in improvement of the heat transfer coefficient in convective heat transfer in nanofluids.

In recent papers, written by Kuznetsov and Nield (2010a,b, 2011a), the Buongiorno's model was applied to the Horton–Rogres–Lapwood problem (the onset of convection in a horizontal layer of a porous medium uniformly heated from below). Both Brownian motion and thermophoresis give rise to cross-diffusion terms that are in some way analogous to the familiar Soret and Dufour cross-diffusion terms that arise with a binary fluid. Nield and Kuznetsov (2011) introduced an analytical treatment of double-diffusive natural convection boundary layer flow in a porous medium saturated by nanofluid. They used the Buongiorno's equation for modeling the nanofluid and Darcy model for porous medium. The result showed a decrease in the reduced Nusselt number associated with an increase in the thickness of the thermal boundary layer an increase in Brownian motion parameter, buoyancy ratio, thermophoresis parameter, modified Dufour parameter, and a decrease in regular buoyancy ratio. The analytical treatment of double-diffusive natural convection boundary layer flow of a nanofluid past a vertical plate was also studied by Kuznetsov and Nield (2011b).

Investigation of force convective heat transfer of nanofluids in a porous channel has not been considered completely in the literature and this challenge is generally considered to be an open research topic that may require more study. The aim of this article is to investigate the effects of particle migration on forced convective heat transfer of nanofluid in a porous medium.

2 Mathematical Formulation

The forced convection heat transfer in a two-dimensional channel is investigated by solving the mathematical formulations introduced in this section numerically. The channel is occupied with a saturated porous medium. The nanofluids which is treated as a two-component mixture, is flown in the channel as discussed by Buongiorno (2006).

The fully developed and steady Darcy–Brinkman–Forchheimer (DBF) equation can be used for fluid flow in porous medium. The Brinkman term in this equation represents viscous effects and makes it possible to impose a no-slip boundary condition at the impermeable wall. Many applications of porous media are characterized by high flow velocities. In such cases, it is necessary to account for deviation from linearity in the momentum equation for porous media. This deviation is accounted for by the Forchheimer term representing the quadratic drag which is essential for large particle Reynolds numbers. Strictly speaking, the quadratic drag appears in momentum equation of porous media are due to the large filtration velocities

and the formation of drag because of the solid obstacles. This drag is comparable with the surface friction drag.

For the case of slow flow condition, as shown in Eq. 1, the advection and Forchheimer quadratic drag term do not appear in momentum equation.

$$\frac{\mu_f}{\varepsilon} \nabla^2 u - \frac{\mu_f}{K} u - \rho_f F \frac{\varepsilon}{K^{\frac{1}{2}}} u^2 - \frac{dP}{dx} = 0. \tag{1}$$

The energy and volume fraction equations are given as follows, respectively.

$$(\rho c)_m \frac{\partial T}{\partial t} + (\rho c)_f u \cdot \Delta T = k_m \nabla^2 T + \varepsilon (\rho c)_p \left(D_B \nabla \varphi \cdot \nabla T + \frac{D_T}{T_C} \nabla T \cdot \nabla T \right) \tag{2}$$

$$\frac{\partial \varphi}{\partial t} + \frac{1}{\varepsilon} u \cdot \nabla \varphi = D_B \nabla^2 \varphi + \frac{D_T}{T_C} \nabla^2 T. \tag{3}$$

where k_m is the effective thermal conductivity of a porous medium. The Brownian motion and thermophoretic parameters are shown in the right hand side of Eq. 2. Nield et al. (2003) indicated that the viscous dissipation term was directly proportional to Brinkman number defined as $\frac{\mu U^2 H}{k \Delta T K}$ with k , ΔT and K as conductivity, temperature difference and permeability. This non-dimensional parameter was first defined by Nield et al. (2003). In this study, the order of magnitude of the aforementioned term is negligible in comparing with other terms of the energy equation. In other words, as the temperature difference between wall and nanofluids increased, the viscous dissipation can ignored. This assumption is often made in heat transfer problem in which the temperature (or heat flux) at the surface is the dominate energy source of the system.

The dimensionless parameters can be written as:

$$u^* = \frac{u}{u_0}; y^* = \frac{y}{H}; x^* = \frac{x}{H}; \varphi^* = \frac{\varphi}{\varphi_0}; T^* = \frac{T - T_0}{T_1 - T_0}; t^* = \frac{t u_0}{\sigma H}; \sigma = \frac{(\rho c)_m}{(\rho c)_f}$$

where u_0 is the average velocity in the channel, T_0 and φ_0 are temperature and particle volume fraction at the channel inlet, T_1 is the wall temperature and H is characteristic length of the channel.

The dimensionless form of Eqs. 1–3 can be written as,

$$\nabla^2 u^* - \frac{u^*}{Da} - \frac{\Delta}{\sqrt{Da}} u^{*2} - \frac{1}{Da} \frac{1}{u_0} \frac{K}{\mu_f} \frac{dP}{dx} = 0 \tag{4}$$

$$\frac{\partial T^*}{\partial t^*} + u^* \frac{\partial T^*}{\partial x^*} = \frac{1}{\text{Repr}} \left[\nabla^2 T^* + \frac{\tau}{Le} (\nabla \varphi^* \cdot \nabla T^*) + \frac{\tau}{Le N_{BT}} (\nabla T^* \cdot \nabla T^*) \right] \tag{5}$$

$$\frac{\partial \varphi^*}{\partial t^*} + \frac{\sigma}{\varepsilon} u^* \frac{\partial \varphi^*}{\partial x^*} = \frac{\sigma}{\text{Resc}} \left[\nabla^2 \varphi^* + \frac{1}{N_{BT}} (\nabla^2 T^*) \right] \tag{6}$$

The dimensionless parameters are defined as follows:

$$Da = \frac{K}{H^2 \varepsilon} \tag{7-1}$$

$$\Delta = \frac{\varepsilon^{\frac{3}{2}} F u_0 H}{\nu_f} \tag{7-2}$$

$$N_{bt} = \frac{D_B \varphi_0 T_1}{D_T \Delta T} \tag{7-3}$$

$$Sc = \frac{\mu}{\rho D_B} \tag{7-4}$$

$$Le = \frac{\alpha_m}{D_B \varphi_0} \tag{7-5}$$

$$Re = \frac{u_0 H}{\nu} \tag{7-6}$$

$$Pr = \frac{\nu}{\alpha_m} \tag{7-7}$$

$$\alpha_m = \frac{k_m}{(\rho c)_f} \tag{7-8}$$

$$\tau = \frac{\varepsilon (\rho c)_p}{(\rho c)_f} \tag{7-9}$$

where, Da , Δ , Re , Sc , Pr are Darcy number, inertia parameter, Reynolds, Schmidt and Prantdl numbers, respectively. The parameter Le is nanofluid’s Lewis number. τ is modified particle-density increment and N_{bt} is a modified diffusivity ratio. This parameter can be expressed as the ratio of Brownian diffusion to the thermophoresis diffusion.

3 Boundary and Initial Conditions

The boundary conditions are as follows

$$\begin{aligned} \text{at } y^* = 0 \text{ and } 2 \quad T^* = 1, \varphi^* = 0, u^* = 0 \\ \text{at } x^* = 0 \quad T^* = 0, \varphi^* = 1 \end{aligned} \tag{8}$$

For outlet boundary, the normal gradient of properties along the outlet is zero and the values of all properties at the outlet are interpolated from the computational domain.

$$\text{At the channel outlet, } x^* = 20: \quad \frac{\partial T^*}{\partial x^*} = 0, \frac{\partial \varphi^*}{\partial x^*} = 0 \tag{9}$$

The initial conditions are:

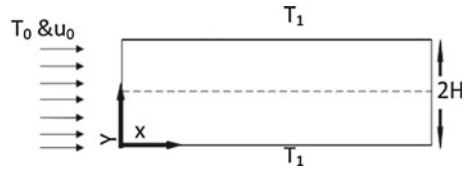
$$T^*(t^* = 0) = 0 \quad \text{and} \quad \varphi^*(t^* = 0) = 0 \tag{10}$$

4 Numerical Method

The finite difference method is used to solve the governing equations appeared in Eqs. 4–6. Fully implicit method is employed to discrete the time dependant terms. It is interesting to notice that the thermophoretic parameter, i.e., ∇T^* , is linearized by the method specified in Patankar 1980. The uniform grids are used in the computational domain. The obtained

Table 1 Grid independency study

Grid Size	Local Nusselt number
100×100	7.5418
200×200	7.5419
300×300	7.542
400×400	7.542

Fig. 1 Geometry of problem and system of coordinate

results are independent of the number of grids. The results of grid independency are given in Table 1. The nonlinear Darcy–Brinkmann–Forchheimer equation is solved by Newton–Raphson method (see, [Epperson 2010](#)). The coupled energy and volume fraction distribution equations are solved by a line-by-line iterative procedure which sweeps the computational domain in $x - y$ directions ([Patankar 1980](#)). The computational procedure for the solution of governing equations can be summarized as follows:

1. Solve the Darcy–Brinkman–Forchheimer equation to obtain the axial velocity (u).
2. Use the obtained velocity and solve the temperature equation to recover the T .
3. Use the new values of T into the volume fraction distribution equation to obtain the new φ .
4. Calculate the absolute error, if $|T^{n+1} - T^n| > 10^{-15}$ and $|\varphi^{n+1} - \varphi^n| > 10^{-15}$, return to step 2 using new φ .

5 Code Validation

The problem inside the channel can be transformed to a simple channel flow problem as the porosity approaches one. In this case the local Nusselt number is calculated and compared with the results of [Shah and London 1978](#) and that of [Bejan 2003](#).

As shown in Fig. 2, the fully developed Nusselt number in the channel with constant wall temperature is 7.54. The fully developed velocity distribution in the porous channel can be obtained analytically as $\Delta \rightarrow 0$. The numerical results in this case, is compared with the analytical Darcy–Brinkman solution. Figure 3a shows the accuracy of the numerical results as the inertial parameter approaches zero.

Finally, the numerical solution of Darcy–Brinkman–Forchheimer model is validated by the analytical solution of [Kuznetsov \(1998\)](#). In this case, a fully developed forced convection in a composite channel bounded by a doubly infinite fixed plates is considered. A porous material is attached to the walls of the channel, while the center of the channel is occupied by a clean fluid. Dimensionless half thickness of the clean fluid region is set to 0.25 (see [Kuznetsov \(1998\)](#)). To describe the flow in the porous region, a momentum equation which accounts for both Brinkman and Forchheimer extensions of the Darcy law is utilized.

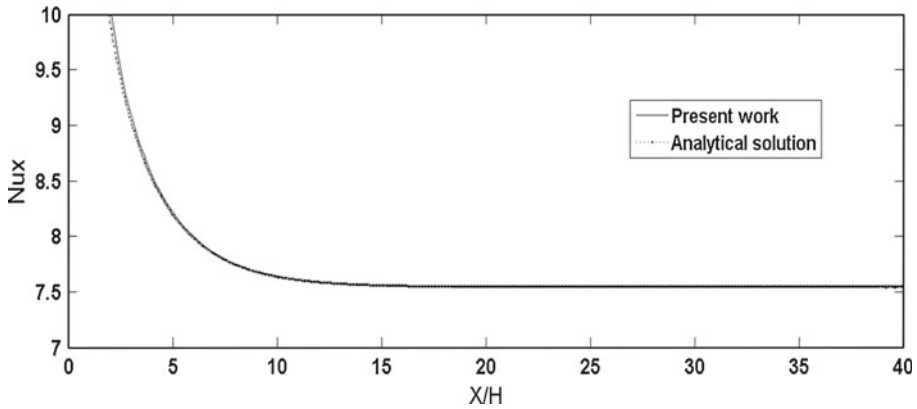


Fig. 2 Comparison of local Nusselt number in this study and analytical solution, as $\varepsilon \rightarrow 1$

Figure 3b shows very good agreement between the numerical and analytical solutions. Figure 3b depicts the distributions of dimensionless velocity, u^* , between the center of the channel and the wall. As expected, velocity increases with an increase in Darcy number.

6 Results and Discussions

In his article, the results related to Eqs. 4, 5, and 6 corresponds to $Pr = 1$, $Re = 1354$, $Da = 1/500$, $\frac{\Delta}{\sqrt{Da}} = 20$, $\tau = 1$ and $\frac{1}{Da} \frac{1}{u_0} \frac{K}{\mu_f} \frac{dP}{dx} = -2$. Figure 4 shows the effects of Lewis number on local Nusselt number, temperature distribution and volume fraction distribution, respectively. As shown in this figure, the Lewis number varies in the range of $100-10^6$ and the results are obtained for $N_{bt} = 0.1$ and $Sc = 100$. The local Nusselt number in the channel is shown in Fig. 4a. It is obvious that for $x^* > 20$, the Nusselt number remains constant and it introduces the thermally developed region inside the porous channel. The volume fraction distribution and temperature profile are shown in Figs. 4b, c in the thermally fully developed region of the channel (at $x^* = 20$). The results show that the local Nusselt number is decreased by increasing the Lewis number. As Eq. 7-5 suggested, any decrease in Brownian diffusion coefficient (D_B) leads to an increase in Lewis number. For preserving N_{bt} constant the denominator of Eq. 7-3 should decrease as D_B decreased. In other words, thermophoretic diffusion coefficient (D_T) should be decreased to keep N_{bt} unchanged.

The volume fraction distribution does not have a significant effect with a change in Lewis number (see Fig. 4b). The governing equations suggest that the energy equation is affected by Lewis number. Therefore, the local Nusselt number and temperature distributions are influenced by the variation of Lewis number. The temperature gradient near the wall is decreased as Lewis number increased and as a result the local Nusselt number decreased. In large Lewis numbers, Eq. 5 is simplified to a classical channel-flow energy equation without the effects of Brownian motion and thermophoresis. As a consequence, in large Lewis numbers, the Nusselt number remains the same as that of a 2D-channel flow occupied by a porous medium.

Because of thermophoresis and Brownian diffusion, particles migrate away from the vicinity of wall to the center of the channel. Figure 5 displays the effect of N_{bt} on local Nusselt number, temperature distribution, and volume fraction distribution. This parameter can be

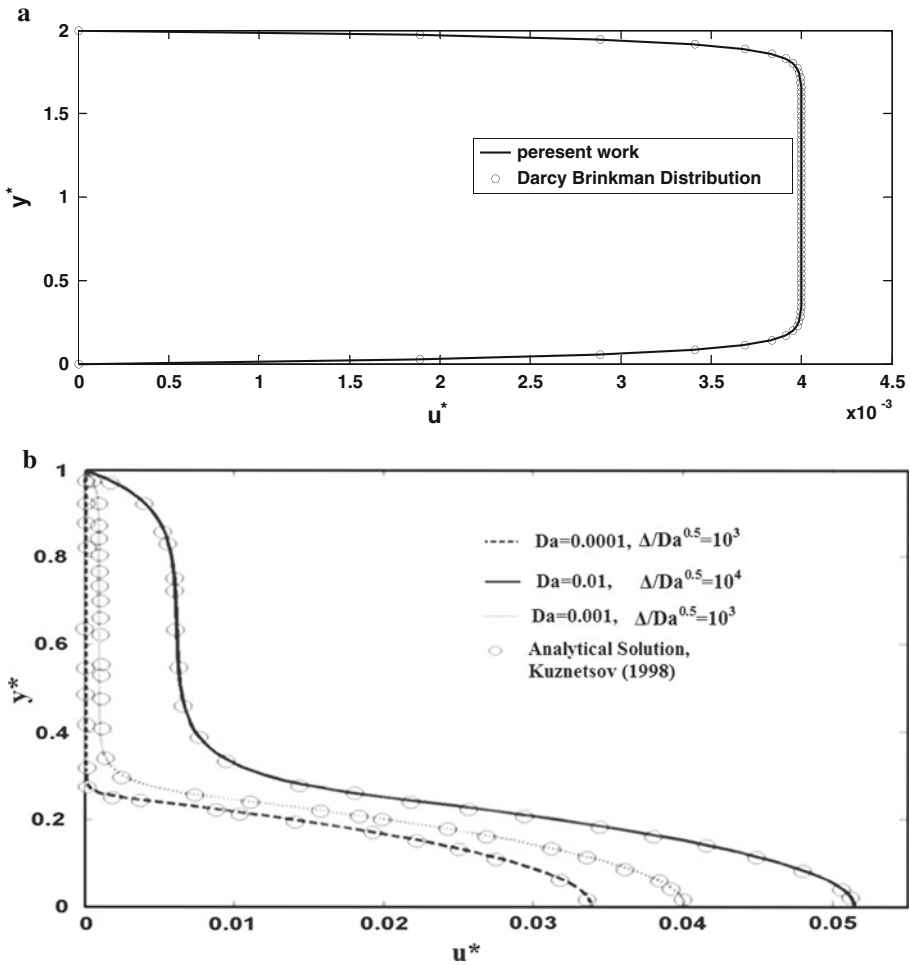


Fig. 3 a Comparison of numerical results and Darcy–Brinkman velocity profile as $\Delta \rightarrow 0$. b Darcy–Brinkman–Förchheimer velocity profile of Kuznetsov and present work comparison

expressed as the ratio between Brownian diffusion to the thermophoresis diffusion. N_{bt} varies within the range of 0.1–0.5. The Schmidt and Lewis numbers are also set to 100. Figure 5a shows the dimensionless volume fraction distribution for different values of N_{bt} . As the wall has the highest temperature, the particles have a tendency to migrate to the channel center. In other words, at a fixed D_B , or constant Lewis and Schmidt numbers based on Eqs. 7-4 and 7-5, an increase in thermophoretic parameter (D_T) results in particle migration to the center of channel. As Eq. 7-2 indicates, an increase in D_T has the same effect as a decrease in N_{bt} . Therefore, any decrease in N_{bt} causes particles to migrate to the center of the channel. Figure 5a, shows this concept completely. A decrease in N_{bt} (i.e., increasing the thermophoretic parameter) leads to an increase in the volume fraction of particles at a specific location inside the channel.

Figure 5b, c shows the dimensionless temperature distribution and the local Nusselt number in the channel for different values of N_{bt} . The results in Fig. 5c indicates that the local

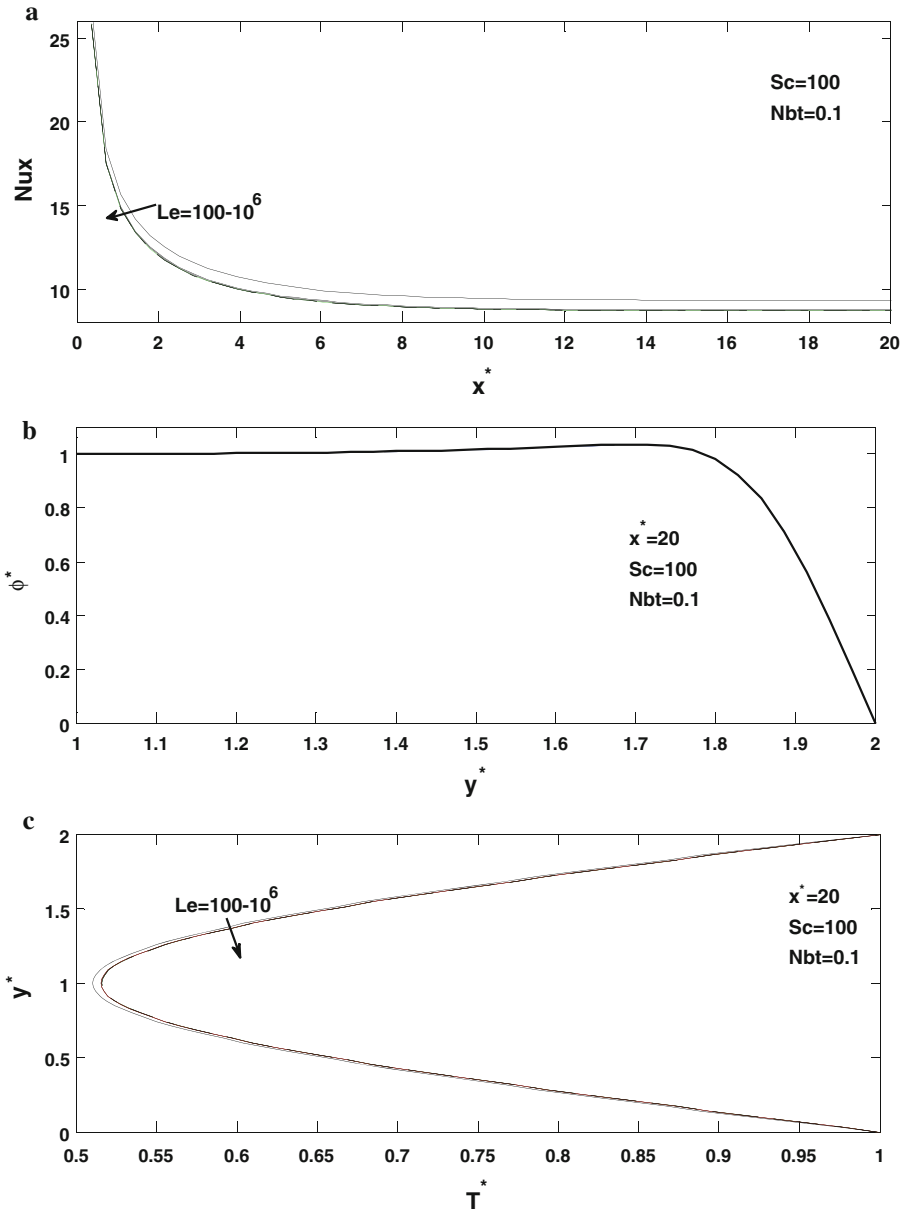


Fig. 4 a Local Nusselt number in the channel for different Lewis numbers. b Dimensionless volume fraction distribution at $x^* = 20$ for different Lewis numbers. c Dimensionless temperature distribution for different Lewis numbers

Nusselt number is decreased as N_{bt} increased. It is interesting to notice that any increase in N_{bt} , leads to a decrease in the gradient of fluid temperature at the wall, and therefore a decrease in Nusselt number.

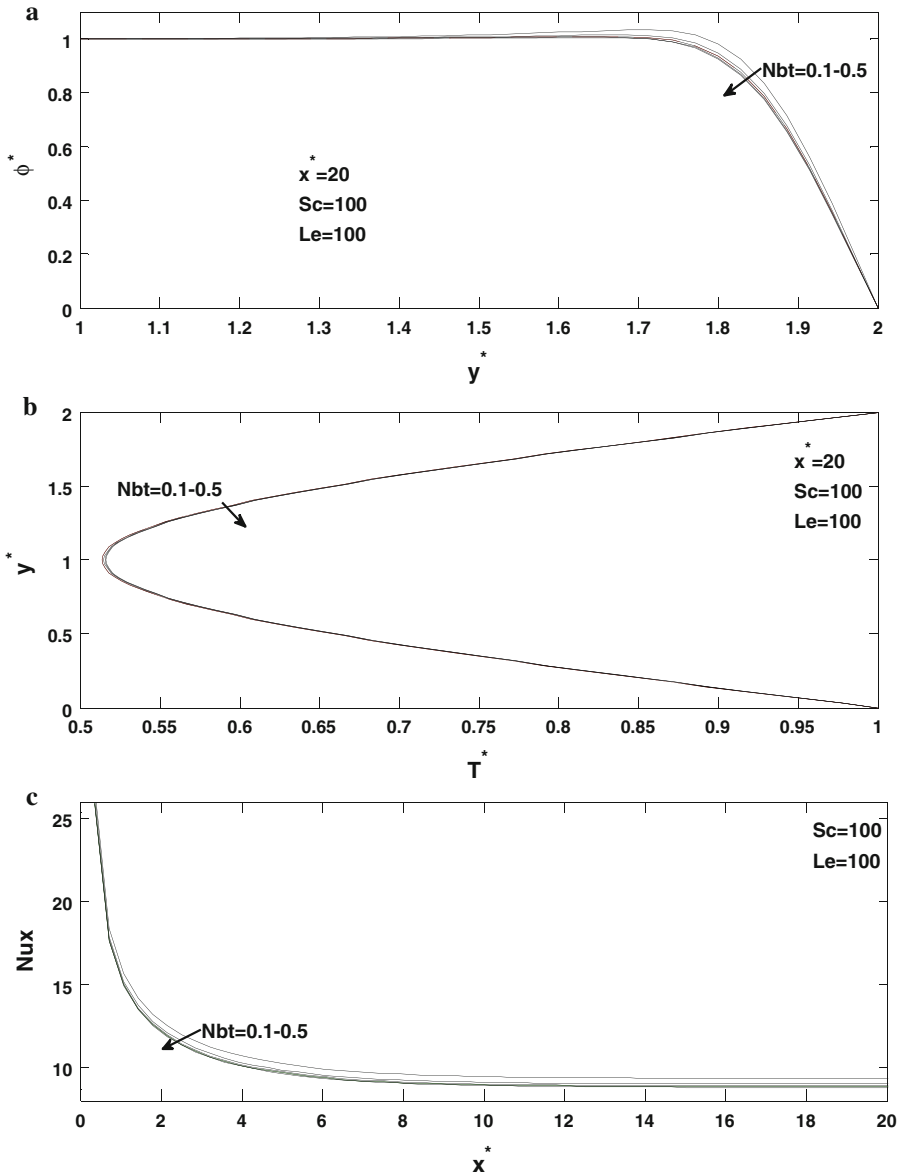


Fig. 5 a Dimensionless volume fraction distribution for different N_{bt} numbers. b Dimensionless temperature distribution for different N_{bt} numbers. c Local Nusselt number for different N_{bt} numbers

Results indicate that when Lewis and Schmidt numbers are not very large, the local Nusselt number and temperature distribution have changed considerably. In contrast, for large values of and Schmidt numbers, the local Nusselt number and temperature distribution curves do not indicate a significant change with N_{bt} . When the Lewis number has a large value, the source terms in the energy equation (i.e., The Brownian motion and thermophoresis terms) can be neglected, and then a classical energy equation is obtained. In this case, the local

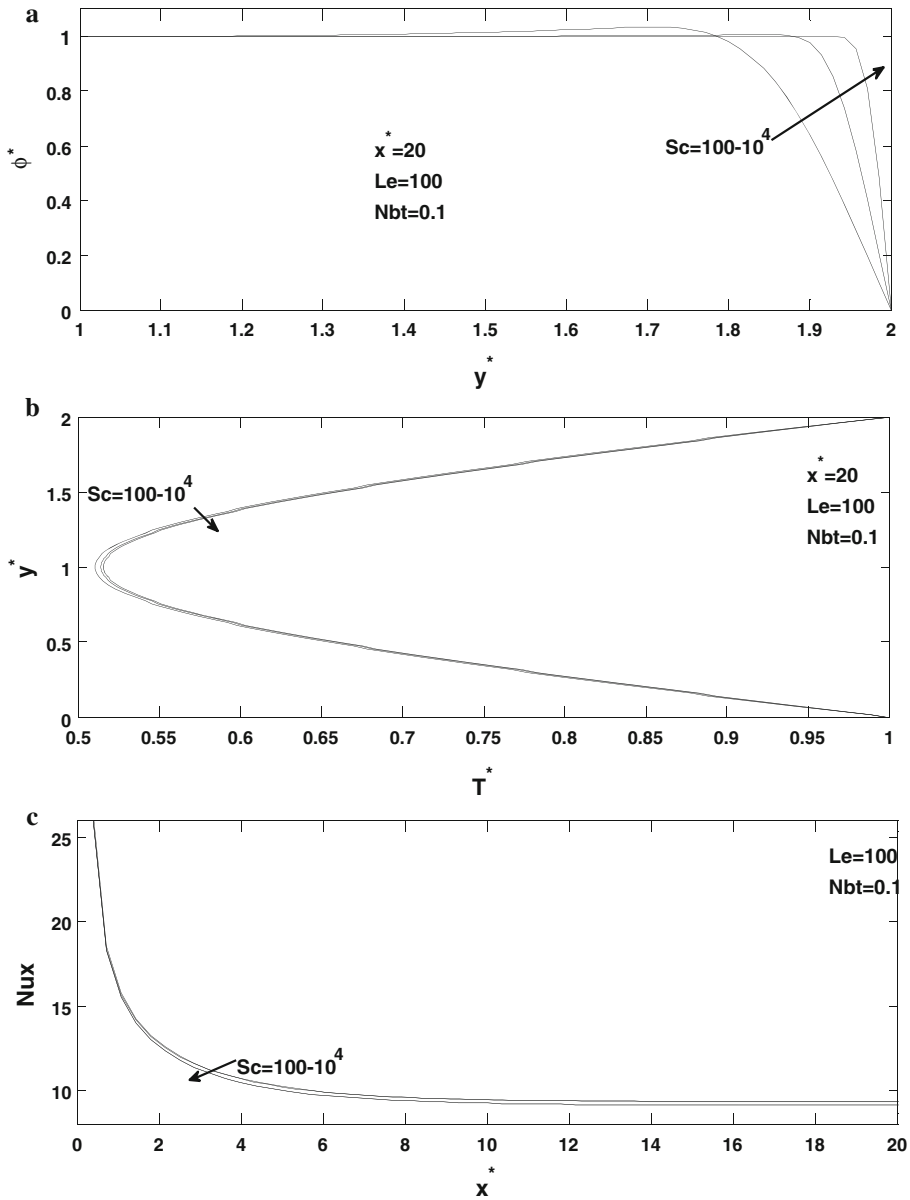


Fig. 6 a Dimensionless volume fraction distribution for various Schmidt numbers. b Dimensionless temperature distribution for various Schmidt numbers. c Local Nusselt number for various Schmidt numbers

Nusselt number and temperature distribution do not have a remarkable change by variation of other parameters like N_{bt} .

Figure 6 shows the effects of Schmidt number which varies within the range of $100-10^4$. N_{bt} and the Lewis numbers are fixed at 0.1 and 100, respectively. When the Schmidt number is increased, the right hand side of Eq. 6 is decreased so the effects of Brownian motion and

thermophoresis are vanished. As shown in Fig. 6a, at large Schmidt number, the convective term is dominated and the volume fraction distribution inside the channel behaves similar to the inlet volume fraction distribution. Figure 6b shows the temperature distribution in the channel. In Fig. 6c it is observed that by an increase in Schmidt number, both the wall temperature gradient and the local Nusselt number are decreased.

7 Conclusion

The effect of particle migration on flow and the heat transfer of nanofluids flowing through a 2-D. porous channel is investigated numerically. The results are given for different Lewis numbers, Brownian motion parameters and Schmidt numbers. The results show a decrease in the local Nusselt number in the porous channel as the Lewis number increased. The local Nusselt number is also decreased by an increase in N_{bt} . The volume fraction distribution does not have a significant change with variation of Lewis number. Decreasing N_{bt} (and as a consequence increasing the thermophoretic parameter) leads to an increase in volume fraction of particles in the channel. In other words, it causes the particles to migrate to the center of channel. At large Schmidt numbers, the convective term is dominant and the volume fraction distribution behaves similar to the inlet volume fraction distribution. It is also observed that as the Schmidt number is increased, the local Nusselt number decreased.

References

- Behzadmehr, A., Saffar-Avval, M., Galanis, N.: Prediction of turbulent forced convection of a nanofluid in tube with uniform heat flux using a two phase approach. *Int. J. Heat Fluid Flow* **28**, 211–219 (2007)
- Bejan, A.: Convective heat transfer, 3rd edn. Wiley, Hoboken (2003)
- Buongiorno, J.: Convection transport in nanofluid. *ASME J. Heat Transf.* **128**, 240–250 (2006)
- Choi, S.U.S.: Enhancing thermal conductivity of fluid with nanoparticles. *Dev. Appl Non-Newtonian Flows* **66**, 99–105 (1995)
- Duangthongsuk, W., Wongwises, S.: Heat transfer enhancement and pressure drop characteristics of TiO₂-water nanofluid in a double-tube counter flow heat exchangers. *Int. J. Heat Mass Transf.* **52**, 2059–2067 (2009)
- Epperson, J.F.: An introduction to numerical methods and analysis. Wiley, Oxford (2010)
- Heris, S.Z., Etemad, S.Gh., Esfahani, M.N.: Experimental investigation of oxide nanofluid laminar forced flow convective heat transfer. *Int. Comm. Heat Mass Transf.* **33**, 529–535 (2006)
- Heyhat, M.M., Kowsary, F.: Effect of particle migration on flow and convective heat transfer of nanofluids flowing through a circular pipe. *ASME J. Heat Transf.* **132**, 062401 (2010)
- Kuznetsov, A.V.: Analytical study of fluid flow and heat transfer during forced convection in a composite channel partly filled with a Brinkman–Forchheimer porous medium. *Flow Turbul. Combust.* **60**, 173–192 (1998)
- Kuznetsov, A.V., Nield, D.A.: Thermal instability in a porous medium saturated by a nanofluid: Brinkman model. *Transp. Porous Media* **81**, 409–422 (2010a)
- Kuznetsov, A.V., Nield, D.A.: Effect of local thermal non-equilibrium on the onset of convection in a porous medium layer saturated by a nanofluid. *Transp. Porous Media* **83**, 425–436 (2010b)
- Kuznetsov, A.V., Nield, D.A.: The effect of local thermal non-equilibrium on the onset of convection in a porous medium layer saturated by a nanofluid: Brinkman model. *J. Porous Media* **14**, 285–293 (2011a)
- Kuznetsov, A.V., Nield, D.A.: Double-diffusive natural convective boundary-layer flow of a nanofluid past a vertical plate. *Int. J. Therm. Sci.* **50**, 712–717 (2011b)
- Lee, J., Mudawar, I.: Assessment of the effectiveness of nanofluid for single-phase and two-phase heat transfer in micro-channels. *Int. J. Heat Mass Transf.* **50**, 452–463 (2007)
- Maiga, S.E.B., Nguyen, C.T., Galanis, N., Roy, G.: Heat transfer behaviors of nanofluid in a uniformly heated tube. *Superlattices Microstruct.* **35**, 453–462 (2004)
- Mirmasoumi, S., Behzadmehr, A.: Numerical study of laminar mixed convection of a nanofluid in a horizontal tube using two-phase mixture model. *App. Therm. Eng.* **28**, 717–727 (2008)

- Nield, D.A., Kuznetsov, A.V., Xiong, M.: Thermally developing forced convection in a porous medium: parallel plate channel with walls at uniform temperature, with axial conduction and viscous dissipation effects. *Int. J. Heat Mass Transf.* **46**, 643–651 (2003)
- Nield, D.A., Kuznetsov, A.V.: The Cheng-Minkowycz problem for double-diffusive natural convective boundary layer flow in a porous medium saturated by a nanofluid. *Int. J. Heat Mass Transf.* **54**, 374–378 (2011)
- Nguyen, C.T., Galanis, N., Polidori, G., Fohanno, S., Pota, C.V., Beche, A.L.: An experimental study of confined and submerged impinging jet heat transfer using Al_2O_3 -water nanofluid. *Int. J. Therm. Sci.* **48**, 401–411 (2009)
- Patankar, S.V.: *Numerical Heat Transfer and Fluid Flow*. Hemisphere, New York (1980)
- Santra, A.K., Sen, S., Chkroborty, M.: Study of heat transfer due to laminar flow of copper–water nanofluid through two isothermally heated parallel plates. *Int. J. Therm. Sci.* **48**, 391–400 (2009)
- Shah, R.K., London, A.L.: *Laminar Flow Forced Convection in Ducts*, supplemental to advances heat transfer. Academic, New York (1978)
- Wang, X.Q., Mujumdar, A.S.: Heat transfer characteristic of nanofluid: a review. *Int. J. Therm. Sci.* **46**, 1–9 (2007)